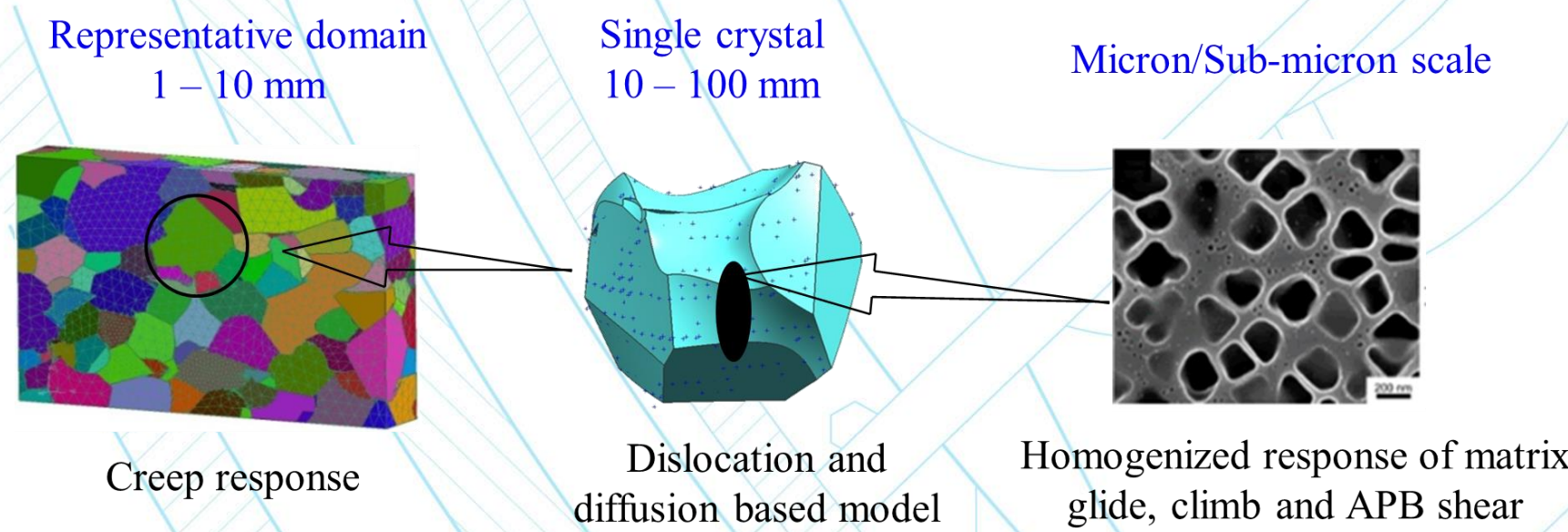


FEA90: Physics-based Creep Simulation of Thick Section Welds in High Temperature and Pressure Applications

Thomas Lillo (PI), Pritam Chakraborty, Wen Jiang – Idaho National Laboratory, Idaho Falls, ID 83415

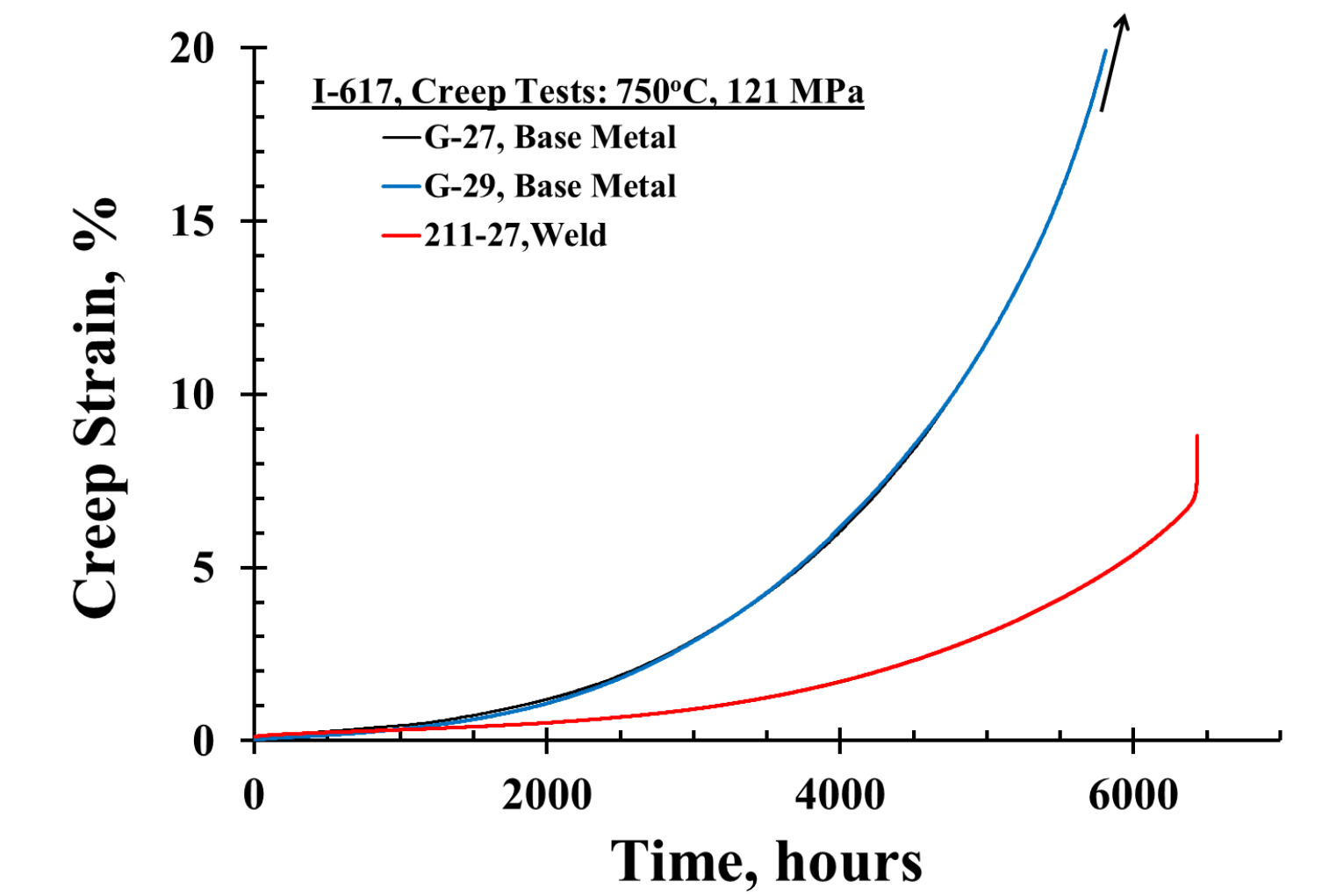
Polycrystalline creep model

- Combination of dislocation and diffusional mechanisms
- Incorporate grain size, shape and orientation effect explicitly
- Homogenized effect of sub-grain features, e.g. precipitate shape, size and volume fraction

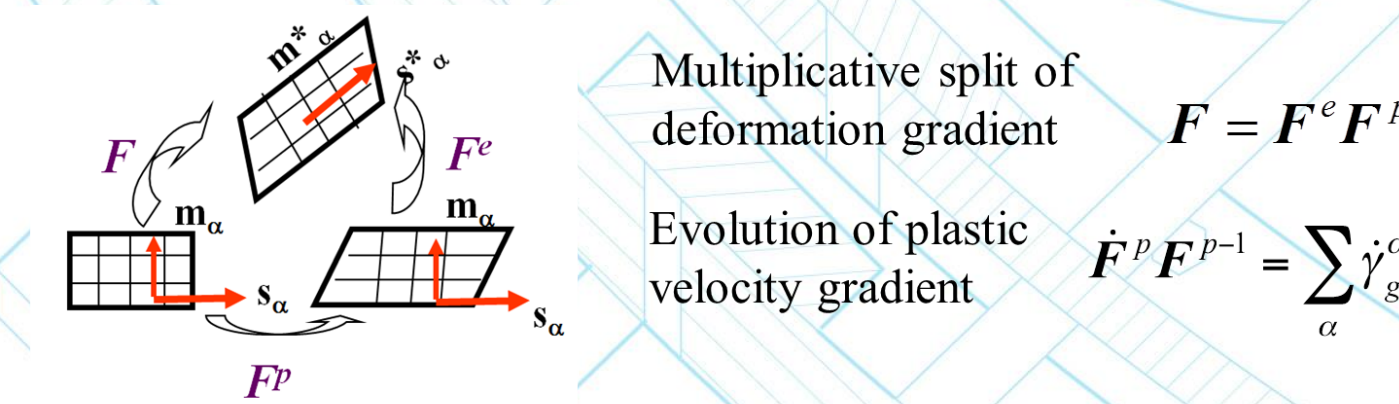


Abstract
Welded microstructures of γ' -strengthened, nickel-based alloys contain significant microstructural heterogeneities that can have a strong influence on the dislocation dynamics, resulting in very different creep behavior compared to the base metal. Crystal plasticity based finite element method (CPFEM) has been widely used to incorporate the effect of microstructural heterogeneities on deformation at the polycrystalline scale and is being utilized in this work to model the creep behavior of the 740H welds. Current model development is focused on secondary creep considering dislocation climb, glide, and anti-phase boundary shearing or Orowan looping. A dislocation-density based CPFEM model addressing these mechanisms is currently being implemented in MOOSE software that provides the ability to solve problems involving multiple physics concurrently and implicitly. The workability of the model is being verified with available Alloy-617 base metal secondary creep data. Short term creep tests at 600-800°C of cross weld and all weld metal samples from ASME-qualified welds in Alloy 740 will be used to determine input parameters for the model. Long term creep tests at 760°C on Alloy 740H welds will be used to validate the results of modeling and simulation.

Alloy 617 Weld Creep Behavior



Dislocation Density Based Crystal Plasticity Model



Glide direction $S_0^\alpha = s^\alpha \otimes m^\alpha$ Climb direction $N_0^\alpha = s^\alpha \otimes s^\alpha$
 s^α - Glide direction m^α - Glide plane normal

Resolved shear stress for glide $\tau^\alpha = T^\alpha : S_0^\alpha$ Resolved shear stress for climb $\tau^\alpha = -T^\alpha : N_0^\alpha$

Dislocation climb model

Equilibrium at dislocation core $\tau^\alpha = -\frac{RT}{V_m} \ln\left(\frac{c^{eq}}{c}\right)$
 R - gas constant; V_m - molar volume; c^{eq} - equilibrium concentration of vacancy at core; c - bulk vacancy concentration;

Climb velocity $v_c^\alpha = -\frac{2\pi D}{b \log(r_c/r_s)} (c^{eq} - c)$ where $r_s = \frac{1}{2\sqrt{\rho_M^\alpha + \rho_I^\alpha}}$
 D - Vacancy diffusion constant; r_c - core radius

Climb rate in matrix $\dot{\gamma}_{c,limb,matrix}^\alpha = (\rho_M^\alpha + \rho_I^\alpha) b v_c^\alpha$

Bulk vacancy evolution $\dot{c} = -\nabla_j + \sum (\rho_M^\alpha + \rho_I^\alpha) b v_c^\alpha$

- All dislocations assumed to be of same character (+)
- Single crystal scale - Absence of explicit precipitate geometry cause $\nabla_j = 0$
- Polycrystal scale - Grain boundary contributes to bulk vacancy evolution $\nabla_j \neq 0$

Evolution of dislocation density

$$\dot{\rho}_M^\alpha = \left(\frac{k_{mult}}{b} \sum \rho^\beta \right) + \left(\frac{2R_c}{b} \rho_M^\alpha \right) + \left(\frac{1}{b\lambda^\alpha} \right) \dot{\gamma}_{glide,matrix}^\alpha + k_{ppt,shar} \rho_I^\alpha \dot{\gamma}_{ppt,shar}^\alpha + k_{c,limb} \rho_I^\alpha \dot{\gamma}_{c,limb,matrix}^\alpha$$

Multiplication, Self-annihilation with opposite signs, Trapping by dislocation and precipitate, Mobilization via APB shear, Mobilization via climb

- Consider immobilization due to matrix dislocation and precipitate
- Climb acts as a bypass and recovery mechanism

Dislocation glide model on a system (α)

$$\dot{\gamma}_{glide}^\alpha = \left(1 - \frac{f_{ppt}}{\rho_I^\alpha}\right) \dot{\gamma}_{glide,matrix}^\alpha + f_{ppt} \dot{\gamma}_{ppt,shar}^\alpha$$

Precipitate volume fraction, Glide in matrix, Precipitate shear by super dislocations

Glide rate in matrix $\dot{\gamma}_{glide,matrix}^\alpha = \rho_M^\alpha b \left[I_g \exp\left(-\frac{\Delta F_g}{kT}\right) \left(1 - \frac{|r^\alpha| - g_{athermal}^\alpha}{g_{thermal}^\alpha}\right)^n \right] \text{sgn}(\tau^\alpha)$; for $|r^\alpha| > g_{athermal}^\alpha$

r_M^α - mobile dislocation density; b - burgers length; I_g - mean free path; n - jump frequency; ΔF_g - activation energy; r^α - resolved shear stress; $g_{athermal}^\alpha$ - athermal resistance; $g_{thermal}^\alpha$ - thermal resistance, p and q - exponents

APB Shear $\dot{\gamma}_{ppt,shar}^\alpha = \rho_M^\alpha b_l v \exp\left(-\frac{\Delta F_p}{kT}\right) \left(1 - \frac{|r^\alpha| - g_{athermal}^\alpha}{g_{thermal}^\alpha}\right) \text{sgn}(\tau^\alpha) \left(k(w_{shar}) \rho_I^\alpha - \rho_c\right)$

r_I^α - immobile dislocation density; I_g - mean free path; ΔF_p - APB energy; $g_{athermal}^\alpha$ - resistive shear stress; k - scaling factor to account for pile up due to precipitate; r_c - critical pile-up

Athermal resistance

$$g_{athermal}^\alpha = Gb \sqrt{q_p \sum A^{\alpha\beta} \rho^{\beta\beta} + q_{ppt} N_{ppt} d_{ppt}}$$

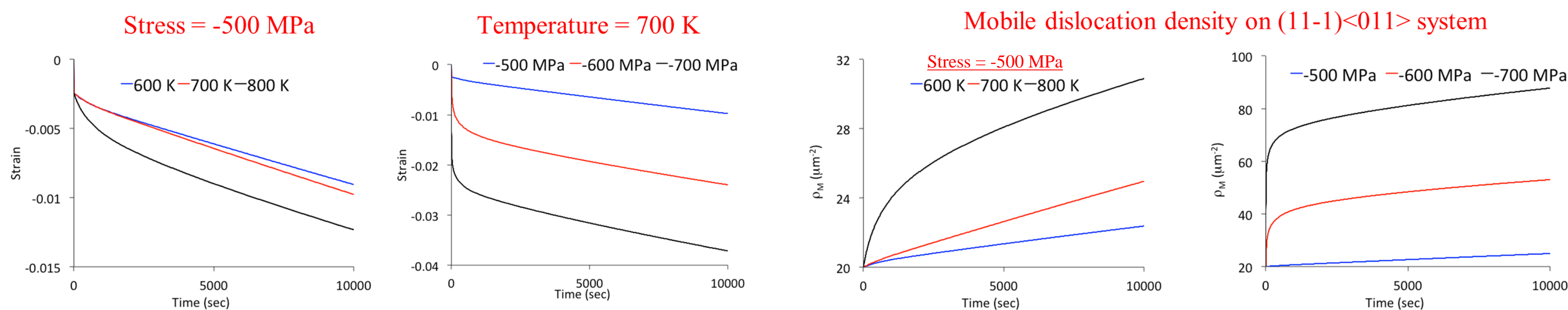
Dislocation-dislocation interaction, Dislocation-precipitate interaction

$A^{\alpha\beta}$ - self and latent hardening; N_{ppt} and d_{ppt} - number density and diameter of precipitates, respectively; q_{ppt} and q_r - constants; G - shear modulus

- Spherical precipitate assumed
- Cuboid shape with $\langle 100 \rangle$ alignment will provide anisotropic resistance

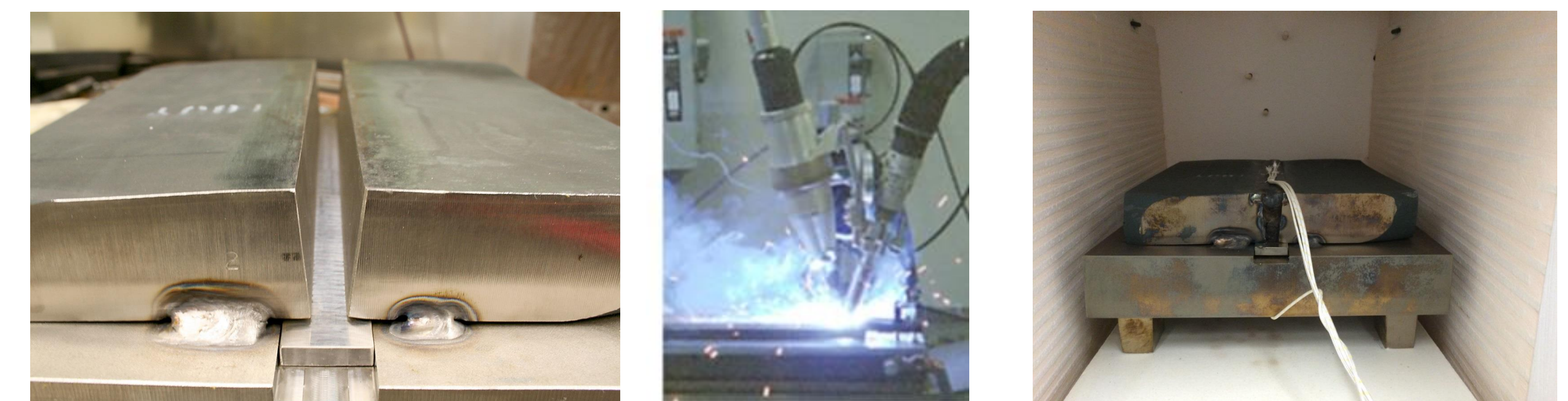
Results

- Implementation of the model in Multi-Physics Object Oriented Simulation Environment software in progress.(MOOSE: mooseframework.org)
- Developed an user-object based plug-n-play system in MOOSE to implement plasticity models efficiently.
- Single crystal simulations performed to test coupled climb and glide (without APB shear and precipitate) models.
- Transition from climb to glide dominated regime achievable by changing stress and temperature.



- Lower stress and temperature, climb rate is higher - lower total creep strain/rate
- Mobile dislocation evolution dominated by mobilization rather than multiplication
- At higher temperature and stress levels, glide rates are significantly higher

ASME-Qualified Welds

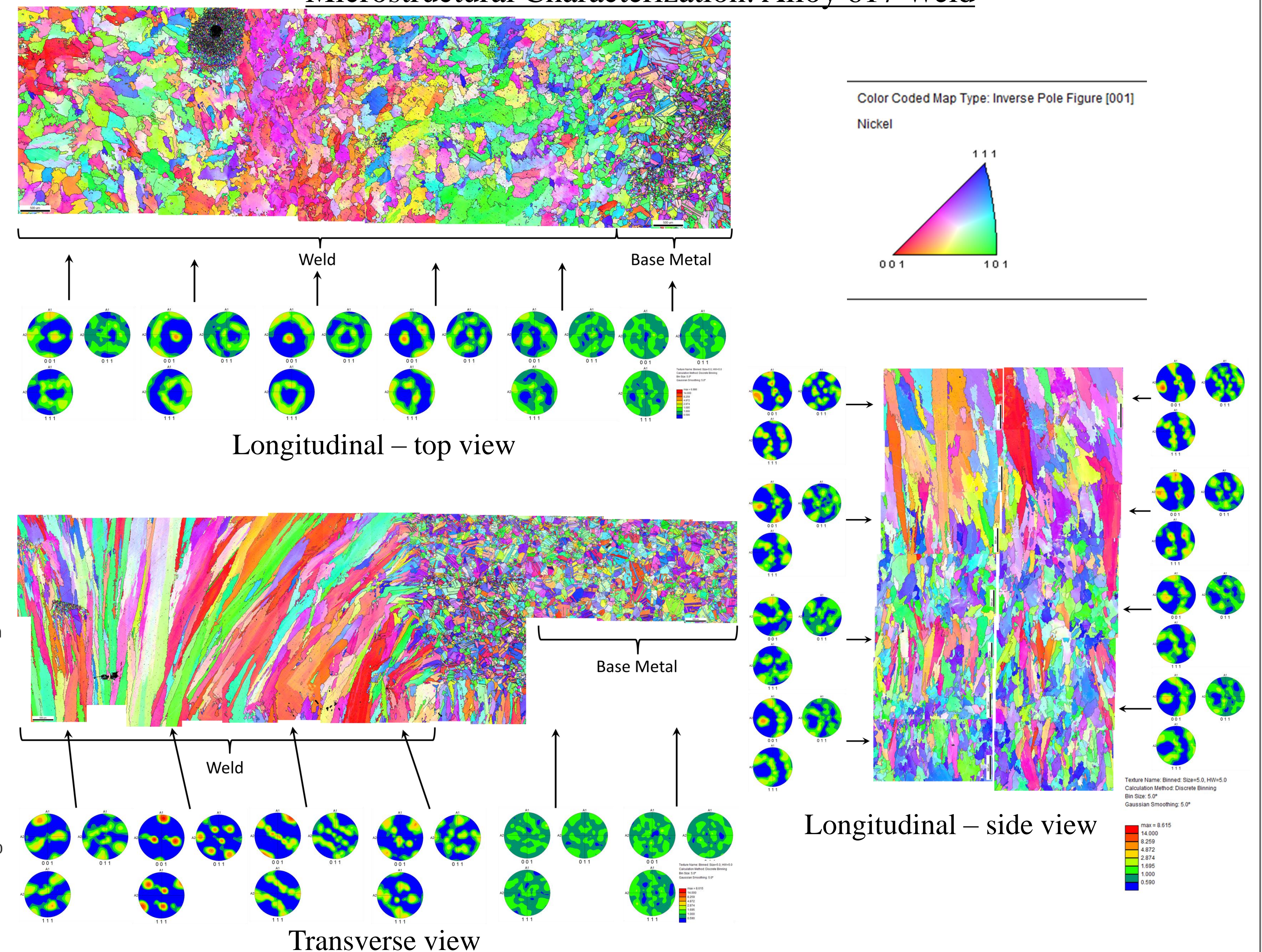


Prior to Welding

Welding

Post-weld Heat Treat

Microstructural Characterization: Alloy 617 Weld



Longitudinal - top view

Longitudinal - side view

Transverse view